

Monitoring Mature Tomato (Red Stage) Quality During Storage Using Ultraviolet-Induced Visible Fluorescence Image

Highlights

- Tomato quality degrades after the red stage, and time after the harvest is important.
- Fluorescence images were tested to monitor quality degradation nondestructively.
- Fluorescence images were effective to monitor tomato storage continuously.
- This approach can be used to monitor tomatoes under a nonideal temperature regime.

1 **Title**

2 **Monitoring Mature Tomato (Red Stage) Quality During Storage Using Ultraviolet-induced**
3 **Visible Fluorescence Image**

4

5 **Author names and affiliations**

6 Keiji Konagaya^a, Dimas Firmanda Al Riza^{a,b*}, Sen Nie^a, Minori Yoneda^a, Takuya Hirata^c, Noriko
7 Takahashi^c, Makoto Kuramoto^d, Yuichi Ogawa^a, Tetsuhito Suzuki^a, Naoshi Kondo^a

8

9 ^a Graduate School of Agriculture, Kyoto University, Kyoto 606-8267, Japan

10 ^b Department of Agricultural Engineering, Faculty of Agricultural Technology, University of
11 Brawijaya, Jl. Veteran 65145, Malang, Indonesia

12 ^c Graduate School of Agriculture, Ehime University, Ehime 790-8566, Japan

13 ^d Advanced Research Support Center, Ehime University, Ehime 790-8577, Japan

14

15 * Corresponding author: dimasfirmanda@ub.ac.id

16

17

18

19

20 **Abstract**

21 The potential of UV-induced fluorescence imaging was investigated as a non-destructive tool to
22 monitor postharvest quality degradation of tomatoes harvested at the red stage and stored at 25°C.
23 The fluorescence images (excitation at 365 nm) were found to be a better indicator of tomato
24 quality degradation than color images after color saturation. Tomatoes were stored at 25 °C for 9
25 d. The changes in color and fluorescence of tomato were evaluated by two types of images: Color
26 and fluorescence images. A conventional colorimeter was also used for as a reference. Changes
27 in the RGB ratio for these two types of images were opposite. In the color images, the G ratio
28 decreased rapidly for the initial 3 or 5 d and then stabilized afterwards. On the other hand, in the
29 fluorescence images, the G ratio increased continuously up to 9 d. Given that temperature
30 conditions during transportation and storage of tomatoes is not always ideal, the results from this
31 research provide the foundation for developing a postharvest monitoring system of mature tomato
32 quality degradation.

33

34 *Keywords:* *Solanum lycopersicum*, storage, fluorescence image, color image, RGB ratio

35

36 **1. Introduction**

37 Tomato (*Solanum lycopersicum*) is one of the most widely consumed agricultural products in
38 the world. Mature red tomatoes taste better, thus peri-urban agriculture often targets the
39 production of these red tomatoes in a number of countries. However, red tomatoes are sensitive
40 to the damage since they are relatively soft compared to greenish tomatoes. Thus, postharvest
41 losses can be an issue. The FAO (2011) reported postharvest losses for fruit and vegetables to be
42 around 10 % worldwide. To minimize these losses, non-destructive quality monitoring of red
43 tomatoes is important. This monitoring would also ensure food safety, and thus benefit both the
44 distribution chain and consumers.

45 Ideally, tomatoes are transported through the distribution chain, right up to the consumers in a
46 cold chain system. However, such a cold chain is not always present during transportation and
47 storage. In developing countries, such as those in Africa, only 10 % of farmers are using a low-
48 cost on-farm cooling system (Arah et al., 2015). This indicates that over 90 % of farmers have no
49 on-farm storage facilities and therefore store their harvested tomatoes at ambient conditions.
50 Furthermore, even such a system does not cover the complete cold chain. The effects on tomato
51 quality during this ambient storage are the target of this study.

52 Tomatoes harvested at the red stage have already attained most of components that contribute
53 to flavor (taste and aroma) (Klee and Giovannoni, 2011). Firmness will, however, continue to
54 decline due to the ripening process. In addition, organic acids will decrease after the red stage,
55 (Chilson et al., 2011), as well as sugars as respiration of the fruit occurs (Fagundes et al., 2015).
56 Thus, total quality, in terms of quality components and firmness, is prone to degradation after
57 the red stage. This is also supported by a drop in sensory ratings after the red stage (Chilson et

58 al., 2011). Monitoring tomato quality degradation after being harvested at the red stage is our
59 focus.

60 One potential method to non-destructively monitor quality degradation of red tomatoes could
61 be color imaging as the tomato becomes a deeper red (Ajlouni et al., 2001). Unfortunately,
62 however, the red color of a tomato saturates during this phase, limiting its capability to monitor
63 quality degradation of red tomatoes.

64 On the other hand, fluorescence, another aspect of color, has the potential to be used for non-
65 destructively monitoring red tomatoes without the above limitation. The fluorescence is light
66 emitted by substance after it is irradiated by light at a shorter wavelength. A number of fluorescent
67 components in tomatoes have been enumerated using high performance liquid chromatography
68 (HPLC). These studies have revealed that red tomatoes contain fluorescent compounds, such as
69 carotenoids (Barba et al., 2006), flavonoids and other phenolic compounds (Slimestad and
70 Verheul, 2009).

71 Some of these compounds are colorless (i.e. pigments that do not absorb light in the visible
72 range) and thus will not be affected by red saturation, as in the color images. Thus, UV-induced
73 fluorescence images could provide unmasked information the color images cannot provide.
74 Furthermore, the content of such compounds have reported to change after being harvested at the
75 light red stage (Toor and Savage, 2006). Thus, UV-induced fluorescence images have the potential
76 to non-destructively monitor tomato quality degradation after the red stage.

77 To date, fluorescence properties of tomato have been studied using multiplex sensors,
78 spectrofluorometers or laser-induced fluorophotometers (Baek et al., 2014; Clément et al., 2015;
79 Hoffmann et al., 2015; Lai et al., 2007). They have demonstrated correlations between

80 fluorescence properties and internal or external qualities associated with ripening in the pre-
81 harvest phase, the existence of cracks or cultivar differences. Hoffmann et al. (2015) also
82 monitored tomatoes during the postharvest storage using fluorescence, but for green harvested
83 tomatoes. Lai et al. (2007) investigated fluorescence properties of red and over-ripe tomato using
84 extraction; a destructive measurement procedure. To the best of our knowledge, no non-
85 destructive procedure for investigating fluorescence component changes in intact mature red
86 tomatoes has been reported.

87 In this study, UV-induced fluorescence images were examined as a non-destructive method
88 with the objective of monitoring quality degradation of tomatoes harvested at the red stage and
89 stored at ambient temperature. These fluorescence images were compared with standard color
90 images, as well as reference values obtained by conventional colorimetry. Tomatoes were stored
91 at 25 °C for 9 d after harvest. The effectiveness of color and fluorescence images were compared
92 in terms of the timing and sensitivity of RGB ratios in these images. The compounds responsible
93 for color and fluorescence images were also discussed based on lycopene content and absorption
94 band position observed in the excitation-emission matrix (EEM).

95

96 **2. Materials and methods**

97 *2.1. Tomato samples*

98 Tomato plants (cultivar Momotaro, currently the most popular in Japan) grown hydroponically
99 in a greenhouse at Ehime University, Matsuyama, Ehime, Japan were used. Details of cultivation
100 are described in a previous study (Takahashi et al., 2018). Tomato seeds were sown on July 21,
101 2017. Seedlings were transplanted to rockwool slabs (Grotop expert, Grodan, Roermond,

102 Netherlands) on September 12, 2017. The plants were irrigated with a nutrient solution containing
103 the following fertilizers; KNO_3 , $\text{Ca}(\text{NO}_3)_2$, $\text{Ca}(\text{NO}_3)_2 \cdot 4\text{H}_2\text{O}$, NH_4NO_3 , H_3PO_4 , KH_2PO_4 , KCl ,
104 K_2SO_4 , $\text{MgSO}_4 \cdot 7\text{H}_2\text{O}$, Fe-EDTA , H_3BO_3 , $\text{MnSO}_4 \cdot 4\text{H}_2\text{O}$, $\text{ZnSO}_4 \cdot 7\text{H}_2\text{O}$, $\text{CuSO}_4 \cdot 5\text{H}_2\text{O}$,
105 $\text{NaMoO}_4 \cdot 2\text{H}_2\text{O}$, at an electrical conductivity of 0.2 S m^{-1} and a pH of 5.5–6.5.

106 Tomatoes (31 fruit in total) were harvested at the onset of the red color stage on June 19, 2018
107 (hue angle < 53.0 and lightness of color (L^*) < 53.0 measured by a colorimeter as described
108 below). Upon harvesting, the fruit were sent to Kyoto University using a commercial delivery
109 service that maintained the tomatoes at $0\text{--}10 \text{ }^\circ\text{C}$ during transportation (24 h period). After arrival,
110 the tomatoes were stored in the dark at $25 \pm 1 \text{ }^\circ\text{C}$ in an incubator (AS ONE Corp., Japan). The
111 relative humidity was maintained at $85 \pm 5 \%$. At each sampling during storage, three or four fruit
112 were used from each day measurement. Sampling occurred at one- or two-day intervals from
113 when the tomatoes were put in storage up to 9 d.

114

115 2.2. Colorimeter

116 For the measurement of L^* , a^* , b^* values a colorimeter CR-200 (Konica Minolta, Inc., Japan)
117 was used under a C illuminant condition. A circle area (8 mm diameter) was measured. The results
118 presented here at each sampling represents the average of four fruit, where each fruit is measured
119 at three locations (once at blossom end and twice at the equator: 180° between positions) were
120 used to obtain an average value for each sample. The error bar represents the standard error (S.E.)
121 of four fruit.

122

123 2.3. Color and fluorescence image

124 For the capture of color and fluorescence images, two light sources and a CMOS camera were
125 used. A schematic diagram of the setup is shown in Fig. 1. The black filled boxes represent the
126 two light sources. The open box represents the camera. For the color images, four halogen lamps
127 (4700 K) were used with a 45° incidence angle to the sample; arranged orthogonal to each other.
128 The average irradiance at 50-mm-height above the sample plane was 2.5 W m⁻². Five C-PL filters
129 (Kenko Tokina Corp., Japan) were also placed in front of the four halogen lamps and the camera
130 to reduce halation with a crossed geometry.

131 For fluorescence image capture, a ring-type 365-nm LEDs (CCS Inc., Japan) were used at a
132 normal incidence. The full width at half maximum (FWHM) for these LEDs was around 10 nm.
133 The average irradiance at the sample plane was 6.9 W m⁻², when placed 190 mm below the light
134 source. To filter out reflected UV light reaching the camera, a long-pass glass filter was placed
135 between the camera and the UV light source (50 % cut at 430 nm). This filter operated as a UV-
136 cut-like filter, but permitted a transmission of 365-nm-light at 0.3%. This ensured two main
137 phenomena (reflection and fluorescence) were observed in the fluorescence image; hereafter
138 referred to as the “fluorescence image”.

139 For both image types, we used a high-resolution CMOS camera EOS Kiss x7 (Canon Inc.,
140 Japan) with parameters set as ISO 100, F-6.3 and shutter exposure 1/25 s and 4 s for both the
141 color and fluorescence images. The camera was calibrated with the same white balance card (X-
142 rite Corp., US).

143

144 *2.4. Analysis of color and fluorescence color*

145 For the analysis of three measurements (a colorimeter, color images and fluorescence images),

146 the RGB values were converted to a ratio (for example $R/(R+G+B)$) by dividing the total intensity
147 of R, G, B channel. This procedure compensates for variations in lightness of color (L^*) and
148 enhances the chromaticity in an arbitrary lightness plane on each day of measurement. The RGB
149 values were further normalized by the mean value at day 1 to compare the performance between
150 the color and the fluorescence images. The RGB ratio was expressed as the mean value with a
151 S.E.

152 For the extraction of RGB values from the two images, a region of interest (ROI) was set. As
153 shown in Fig. 4, there were apparently three different regions at the blossom end: The distal area
154 (d in Fig. 4), vascular bundles (v in Fig. 4) and the other remaining zone. For all analyses, the
155 whole blossom end area except for the distal area was set as the ROI.

156 In detail, the distal area was defined as a circle with a 5-mm diameter. The blossom end area
157 was defined as four ninth of the whole blossom end area (i.e. two thirds of the diameter), after
158 removing the distal area. In case of fluorescence images, the center blue area (10 mm diameter
159 circle) in Fig. 4 was also removed to reduce the effect of reflection of the excitation light. Image
160 analysis was conducted using Image J software (NIH).

161

162 *2.5. Lycopene content*

163 Changes in the images was correlated with the lycopene content of the tomato, which was
164 measured using the method of Ito and Horie (2009). Lycopene was extracted two times with
165 acetone (35 mL and 15 mL). Each tomato was homogenized using a blender (28 fruit in total). An
166 aliquot of the blended tomato, around 1.5 g, was added to 35 mL of acetone and shaken in brown
167 tubes for 10 min. After shaking, the supernatant solution was moved to a brown measuring flask.

168 This extraction procedure was repeated with 15 mL of acetone. After the extraction, the solution
169 was adjusted to 50 mL by adding further acetone to the flask. The solution was filtered using a
170 0.45 μm disposal filter (AS ONE Corp., Japan). The absorbance of the supernatant was measured
171 using a spectrophotometer V-670 (JASCO Corp., Japan). The lycopene concentration was
172 calculated using a molar absorption coefficient of $3150 \text{ \%}^{-1}\text{cm}^{-1}$ at 505 nm in acetone (Nagata et
173 al., 2007), which is the peak wavelength of lycopene. The lycopene content was calculated by
174 dividing the content in the solution by the tomato aliquot mass. The results were expressed in mg
175 kg^{-1} lycopene on a fresh weight basis.

176

177 *2.6. Excitation-emission matrix*

178 To identify potential components associated with changes in the fluorescence images, an
179 excitation-emission matrix (EEM) was measured using a spectrofluorometer FP-8300 (JASCO
180 Corp., Japan). The spectral range of excitation and emission were 250–660 nm and 280–700 nm,
181 respectively. The band width was set to be 5 nm for both slits. The photomultiplier tube (PMT)
182 sensitivity was set to prevent saturation with a response time and scan speed of 50 ms and 5000
183 nm min^{-1} , respectively. Different tomatoes were selected for EEM measurement and image
184 capture. A pericarp slice (20 mm diameter with 3-mm-thick) from the equatorial zone was
185 attached to the sample holder (20-mm diameter quartz window). The incident and detection angles
186 were 30° and 60° , respectively.

187

188 **3. Results**

189 *3.1. Changes in L^*C^*h values and RGB ratio from a colorimeter*

190 To investigate the color changes of tomato from the red stage, L^* , a^* , b^* values were measured
191 by a colorimeter. Previously, the color of tomatoes has been evaluated based mainly on a^* or
192 a^*/b^* (López Camelo and Gómez, 2004; Bui et al., 2010), but more recent studies have also used
193 other color values in the $L^*a^*b^*$ - or L^*C^*h -color spaces. (Dhakal and Baek, 2014; Torres et al.,
194 2015; van Roy et al., 2017). From a human perception perspective, the color expressed in the
195 L^*C^*h -color space is more easily understandable.

196 Fig. 2 shows the hue angle and lightness of tomatoes during the storage at 25 °C. The hue angle
197 and the lightness initially decreased until day 3. The chroma (i.e. saturation in HSI-color space)
198 fluctuated (27.8 ± 1.0 , 29.1 ± 1.4 to 30.2 ± 0.9 for 1, 5 to 9 d). This decreasing trend of hue angle
199 during storage of our red tomatoes was consistent with previous reports for yellow (Pek et al.,
200 2010; Thai et al., 1990) and green (Dhakal and Baek, 2014) tomatoes at harvest. This indicates
201 the decreasing trend of hue angle was consistent regardless of maturity stage at harvest. In
202 $L^*a^*b^*$ -color space, a^* increased until day 5, while b^* decreased rapidly at day 3. The a^*/b^*
203 parameter increased until day 3, being inversely correlated with the hue angle changes, as
204 expected by their mathematical relationship, since hue angle is defined as $\tan^{-1}(b^*/a^*)$. Hue angle
205 and lightness, obtained by the colorimeter, were useful to monitor the quality degradation of
206 tomatoes that were harvested at the red stage and stored at 25 °C until at least day 3.

207 To compare with fluorescence, an optimum wavelength region, in other words, a color channel
208 (R, G, B) is important. To reduce the undesirable effect of lightness and enhance chromaticity
209 (the best estimate of color without intensity), the RGB values were divided by $R+G+B$ and
210 normalized by their initial values for each ratio to compare the performance between the color
211 and fluorescence images.

212 Fig. 3 shows the relative RGB ratios of tomato during storage. The R ratio increased while the
213 G ratio decreased. The B ratio rapidly increased at day 3, decreasing slightly there afterwards.
214 The decrease of hue angle in Fig. 2 is associated with an increase in the R ratio and decrease in
215 the G ratio. This could be due to accumulation of lycopene, which absorbs green light and reflects
216 red light (Choudhary et al., 2009; Zhu et al., 2015). Even though the tomato appears reddish, in
217 color, not only the R ratio, but the G ratio also has the potential to monitor tomato quality
218 degradation when harvested at the red stage and stored at 25 °C until day 5.

219

220 *3.2. Changes in RGB ratio from the color and fluorescence images*

221 The color and fluorescence images of the tomatoes were evaluated using a non-contact image
222 capture system. Fig. 4 shows typical color and fluorescence images of the same tomato. In the
223 color images, the fruit appear to be reddish in color, but the distal area and vascular bundles
224 exhibited a brownish and yellowish color, respectively. Meanwhile, the fluorescence images
225 appear to be bluish overall, but the distal area appears to be whitish, while the vascular bundles a
226 relatively dark blue, suggesting the presence of visible and invisible pigments were unevenly
227 distributed at the blossom end of tomatoes.

228 To quantify the chromaticity values more accurately, changes in RGB ratios from the two types
229 of images were examined for the ROI (the blossom end without the distal area). Fig. 5 shows the
230 relative RGB ratios of tomato during the storage obtained by the color images. In the color image,
231 the R ratio increased, while the G ratio decreased until day 3. These trends are the same as those
232 observed in the colorimeter measurements. The distal area exhibited a relatively unchanging
233 profile except for the G ratio over the entire period (1.00 ± 0.02 to 1.08 ± 0.03 for R ratio, $1.00 \pm$

234 0.05 to 0.79 ± 0.07 for G ratio and 1.00 ± 0.04 to 0.90 ± 0.09 for B ratio). This is associated with
235 the existence of several brownish pigments, suggesting low amounts of lycopene in this area. The
236 color images could effectively monitor tomato quality degradation after being harvested at the red
237 stage and stored at 25 °C up until day 3.

238 As a supplementary or alternative way to monitor tomato quality degradation, fluorescence
239 images were examined. Fig. 6 shows the relative RGB ratios obtained from the fluorescence
240 images. The trend for chromaticity was totally different from the colorimeter and color images,
241 as shown in Figs. 3 and 5. Overall, the R ratio remained relatively unchanged (distal area
242 excluded), while the G ratio increased and the B ratio decreased. Especially, the G ratio of the
243 blossom end (distal area excluded) became higher at day 9. From this, it can be seen that the
244 fluorescence image was sensitive to changes in tomato quality degradation over the entire storage
245 period; much longer time provided by colorimeter and color images. Further details are explored
246 in the discussion section.

247 The distal area was totally different from that of other areas. The most apparent difference was
248 the significantly brighter spot in the distal area, as shown in Fig. 4. Although we hypothesized
249 that this might have been caused by scattering or reflection of the excitation-light, further
250 investigation showed the bright phenomenon occurred irrespective of lighting angle, thus we
251 confirmed that this was caused by fluorescence.

252

253 **4. Discussion**

254 *4.1. Compounds affecting color images*

255 A knowledge of the chemical compounds associated with changes in the color image is

256 important for future applications. The most dominant pigment in tomatoes is lycopene (up to 181
257 mg kg⁻¹), which has a red color (Chaudhary et al., 2018; Martí et al., 2016). Absorption of
258 lycopene in tomatoes is known to peak around 500–550 nm (Zhu et al., 2015); absorbing green
259 blue light, but reflecting red light. This is reflected in the G, B ratios, and the R ratio of the color
260 images. In the current research, lycopene content was moderately correlated with the R ratio of
261 the color images ($r=0.81$), as shown in Fig. S1. The correlations with G and B ratio were negative;
262 $r=-0.80$ and $r=-0.67$, respectively. This suggests that while lycopene content of lycopene is a
263 major contributor, it does not explain all the variation.

264 Another group of pigments, carotenoids, are also known to contribute to color image
265 differences in tomato, with up to 12 mg kg⁻¹ of β -carotene (Chaudhary et al., 2018; Martí et al.,
266 2016); orange in color. The absorption characteristics of β -carotene are almost the same as those
267 of lycopene with the same basic 11-isoprenes structure; the main difference being a slight blue-
268 shift (Meléndez-Martínez et al., 2019). However, the content of β -carotene is only a small
269 percentage of total carotenoid content (Martí et al., 2016). Thus, the contribution is relatively low.

270 Other carotenoids, such as phytoene and phytofluene are known to be precursors of lycopene
271 and carotenes (Meléndez-Martínez et al., 2015), but their absorption maxima are around 280 and
272 350 nm in petroleum ether, respectively (Meléndez-Martínez et al., 2019), thus they are colorless
273 and not visually apparent in the color images. Another possible pigment affecting the color images
274 is naringenin chalcone (up to 182 mg kg⁻¹) (Martí et al., 2016), which is yellow. Naringenin
275 chalcone absorbs purple light, thus it also might affect the B ratio of the color image.

276

277 *4.2. Changes in color images*

278 As indicated in the discussion above, lycopene is considered to be the component most closely
279 associated with changes in the postharvest color images. Fig. 7 documents the measured changes
280 in lycopene content during storage. Lycopene content increased from the start of storage from
281 37.3 ± 2.8 to 99.7 ± 3.7 mg kg⁻¹ at day 5, stabilizing until day 7, and then slightly increasing again
282 up to 115.8 ± 9.9 mg kg⁻¹ at day 9. The overall trend was consistent with the observed changes in
283 the RGB ratios of the color images, suggesting that lycopene is one of the most predominant
284 pigment contributing to changes in the color images of the tomatoes in our storage condition.

285

286 *4.3. Compounds affecting fluorescence images*

287 The compounds associated with changes in the fluorescence images were inferred from the
288 EEM. Fig. 8 shows a typical EEM of a 3-mm-thick slice of tomato before and after storage. No
289 fluorescent peaks were observed in the visible region with excitation wavelengths used. This
290 means that any fluorescent compounds present are colorless to the naked eye.

291 In the EEM, there were two main excitation peaks at 250 and 360 nm with an emission at
292 around 420 nm, for both excitations. These two peaks were highly correlated ($r=0.91$), as shown
293 in Fig. S2. This indicates the two peaks are derived from the same compounds, although there
294 might be another minor contribution from a different compound with an excitation at 250 nm, as
295 suggested by the negative intercept of 25 counts out of a total count of 50–120 (i.e. 20–50 % of
296 total intensity comes from other minor compounds). Fig. S3 shows the excitation and emission
297 spectra of all tomatoes measured (28 fruit). The excitation spectra had two peaks, indicating the
298 compounds have two vibration structures. The most likely compounds that meet this criteria are
299 phenolics (including flavonoid and some longer phenolic acid) or some vitamins, which exist in

300 tomato (Chaudhary et al., 2018). We tentatively assigned the excitation peak at 350 nm to a
301 flavonoid, consistent with that assigned by Lai et al. (2007).

302 There are also potential fluorescent compounds contributing to the observed excitation peaks.
303 Carotenoids (i.e. phytoene and phytofluene) and simple phenolics with one aromatic ring (i.e.
304 some amino acid and shorter phenolic acid) are other major groups known to have an absorption
305 in the observed excitation range. But in the case of such compounds, only one absorption band
306 would be expected between 250 and 600 nm of excitation, which contradicts the measured
307 excitation spectra (Fig. S3).

308 Furthermore, carotenoids including lycopene (Song and Moore, 1974) and β -carotene (Gillbro
309 and Cogdell, 1989; Song and Moore, 1974) are known to have extremely low quantum yields of
310 less than 1×10^{-4} , compared to flavonoids $0.2\text{--}23 \times 10^{-3}$ (Park et al., 2013) and other simple
311 phenolics 0.01–0.1 (Wünsch et al., 2015). In addition, we could not find any fluorescence peak
312 of lycopene in the measured EEM (Fig. 8). Lemos et al. (2015), who compared a lycopene
313 standard with tomato extract, also could not find any lycopene fluorescence peak. This strongly
314 suggests the fluorescent compounds observed in the fluorescence images are colorless pigments,
315 except for carotenoids.

316

317 *4.4. Changes in fluorescence images*

318 In the EEM, excitation at 250 and 360 nm resulted in similar fluorescence emission spectra
319 from tomatoes during storage (Fig. 9). In the spectra, there was a transition point at around 430
320 nm, with relative intensity decreasing below 430 nm and increasing above 430 nm during storage.

321 This was consistent with observed decreases in the B ratio and increases in the R and G ratios of

322 the fluorescence image (Fig. 6).

323 Furthermore, several phase changes occurred in the observed fluorescence over time. From
324 days 1 to 3, the change was small, which corresponded with slight changes in the G ratio over the
325 same period (Fig. 6). Then, from days 3 to 5, there was a jump in emissions above 430 nm, with
326 a corresponding slight increase in the G ratio (Fig. 6), followed by a stable period between days
327 5 to 7, and then another period of increase from days 7 to 9. In the later period, there was not only
328 a broadening, but also a peak shift around 470 nm. The second increase in the G ratio from days
329 7 to 9 might be affected by the two phenomena: broadening and shift of the emission spectra. This
330 suggests at least two separate phenomena occurred with the fluorescent compounds, such as
331 changes in the surrounding environment and the relative concentrations of these compounds,
332 resulting in the broadening and the peak shift, respectively.

333 The RGB ratios of fluorescence images changed (Fig. 6) after the saturation of the RGB ratios
334 in the color images (Fig. 5). This suggests that the changes in the fluorescent compounds were
335 initiated after saturated accumulation of lycopene occurred. Since the ripening is the well
336 programmed phenomenon controlled by the numerous genes, one hypothesis is the fluorescent
337 compounds are regulated by the carotenoid-related genes such as PSY1, PDS and ZDS (Osorio
338 et al., 2012). However, there was low correlation between the peak maxima at 250 and 360 of
339 excitation with the lycopene content with correlation coefficient of -0.21 and -0.17 nor with the
340 fluorescence emission ratio (460 nm/420 nm at the excitation of 360 nm) with correlation
341 coefficient of 0.54. The changes in the fluorescent compound responsible for the fluorescence
342 image was unrelated with the lycopene accumulation.

343 We acknowledge there are several limitations in this work. First, we could not investigate the

344 optimum color spaces, white balance setting or correction of RGB sensitivity in the camera
345 capturing the fluorescence images. However, since the absolute value of fluorescence emissions
346 was difficult to standardize, the relative values were effective for our monitoring purposes.
347 Second, we have not directly identified the compounds associated with the quality changes
348 observed in the fluorescence images. In future work, we need to elucidate the mechanisms behind
349 the fluorescent phenomena. This mechanism would answer what metabolic pathways were
350 visualized in relation to the synthesis and degradation of the fluorescent compounds near the
351 surface.

352

353 **5. Conclusions**

354 In this study, we investigated the potential of UV-induced fluorescence images to non-
355 destructively monitor quality degradation of tomato after being harvested at a red stage and stored
356 at 25°C. Fluorescence imaging (using excitation at 365 nm) was found to be sensitive to tomato
357 quality degradation for a longer period during storage than color imaging. In color and
358 fluorescence images, the observed trends were opposite. In color images, the G ratio rapidly
359 decreased for the first 3 to 5 d, but after this, values became saturated. On the other hand, in
360 fluorescence images, the G ratio increased continuously up to 9 d for tomatoes stored at 25 °C.

361 In future, we plan to investigate the application of this technique to monitoring of tomatoes
362 harvested at different maturity stages, under different storage temperatures, harvesting seasons,
363 cultivars and growth treatments. The identification of fluorescence compounds will also need to
364 be included in future research work. Since in the postharvest period tomatoes are often transported
365 and stored at least than ideal temperatures, this study demonstrates that fluorescence imaging can

366 be used as a monitoring system of mature tomato quality degradation following harvesting right
367 through to consumption.

368

369 **Declaration of interest:** none.

370

371 **Acknowledgements**

372 We thank Ms. Annisa Nurulhuda for the important preliminary study. We are also grateful to
373 Mr. Miah Sumon, Dr. Muharfiza (Ministry of Agriculture, Indonesia), Ms. Mayumi Kanayama,
374 Ms. Hikari Nishio for technical supports. We also acknowledge Dr. Garry John Piller (Kyoto
375 University) for his help and useful discussions. Financial support was provided by Matsushima
376 Horticultural Development Foundation, Japan.

377

378 **References**

- 379 Ajlouni, S., Kremer, S., Masih, L., 2001. Lycopene content in hydroponic and non-hydroponic
380 tomatoes during postharvest storage. *Food Aust.* 53, 195–196.
- 381 Arah, I.K., Kumah, E.K., Anku, E.K., Amaglo, H., 2015. An overview of post-harvest losses in
382 tomato production in Africa: Causes and possible prevention strategies. *J. Biol.* 5, 78–88.
- 383 Baek, I.-S., Kim, M., Lee, H., Lee, W.-H., Cho, B.-K., 2014. Optimal fluorescence waveband
384 determination for detecting defective cherry tomatoes using a fluorescence excitation-
385 emission matrix. *Sensors* 14, 21483–21496. <https://doi.org/10.3390/s141121483>
- 386 Barba, A.I.O., Hurtado, M.C., Mata, M.C.S., Ruiz, V.F., Tejada, M.L.S. de, 2006. Application
387 of a UV–vis detection-HPLC method for a rapid determination of lycopene and β -carotene in

388 vegetables. Food Chem. 95, 328–336. <https://doi.org/10.1016/j.foodchem.2005.02.028>

389 Bui, H.-T., Makhlof, J., Ratti, C., 2010. Postharvest ripening characterization of greenhouse
390 tomatoes. Int. J. Food Prop. 13, 830–846. <https://doi.org/10.1080/10942910902895234>

391 Chaudhary, P., Sharma, A., Singh, B., Nagpal, A.K., 2018. Bioactivities of phytochemicals
392 present in tomato. J. Food Sci. Technol. 55, 2833–2849. [https://doi.org/10.1007/s13197-018-](https://doi.org/10.1007/s13197-018-3221-z)
393 3221-z

394 Chilson, D., Delgado, A., Cecilia, M., Nunes, N., 2011. Shelf life of cluster tomatoes
395 (*Lycopersicon esculentum*) stored at a non-chilling temperature and different relative
396 humidity levels, in: Proc. Fla. State Hort. Soc. pp. 246–255.

397 Choudhary, R., Bowser, T.J., Weckler, P., Maness, N.O., McGlynn, W., 2009. Rapid estimation
398 of lycopene concentration in watermelon and tomato puree by fiber optic visible reflectance
399 spectroscopy. Postharvest Biol. Technol. 52, 103–109.
400 <https://doi.org/10.1016/j.postharvbio.2008.10.002>

401 Clément, A., Bacon, R., Sirois, S., Dorais, M., 2015. Mature-ripe tomato spectral classification
402 according to lycopene content and fruit type by visible, NIR reflectance and intrinsic
403 fluorescence. Qual. Assur. Saf. Crops Foods 7, 747–756.
404 <https://doi.org/10.3920/QAS2014.0521>

405 Dhakal, R., Baek, K.-H., 2014. Short period irradiation of single blue wavelength light extends
406 the storage period of mature green tomatoes. Postharvest Biol. Technol. 90, 73–77.
407 <https://doi.org/10.1016/j.postharvbio.2013.12.007>

408 Fagundes, C., Moraes, K., Pérez-Gago, M.B., Palou, L., Maraschin, M., Monteiro, A.R., 2015.
409 Effect of active modified atmosphere and cold storage on the postharvest quality of cherry

410 tomatoes. *Postharvest Biol. Technol.* 109, 73–81.

411 <https://doi.org/10.1016/j.postharvbio.2015.05.017>

412 FAO, 2011. Global food losses and food waste – Extent, causes and prevention. Food and
413 Agriculture Organization of the United Nations, Rome.

414 Gillbro, T., Cogdell, R.J., 1989. Carotenoid fluorescence. *Chem. Phys. Lett.* 158, 312–316.

415 [https://doi.org/10.1016/0009-2614\(89\)87342-7](https://doi.org/10.1016/0009-2614(89)87342-7)

416 Hoffmann, A.M., Noga, G., Hunsche, M., 2015. Fluorescence indices for monitoring the
417 ripening of tomatoes in pre- and postharvest phases. *Sci. Hortic.* 191, 74–81.

418 <https://doi.org/10.1016/j.scienta.2015.05.001>

419 Ito, H., Horie, H., 2009. Proper solvent selection for lycopene extraction in tomatoes and
420 application to a rapid determination. *Bull. Natl. Inst. Veg. Tea Sci. Jpn.* 8, 165–173.

421 Klee, H.J., Giovannoni, J.J., 2011. Genetics and control of tomato fruit ripening and quality
422 attributes. *Annu. Rev. Genet.* 45, 41–59. [https://doi.org/10.1146/annurev-genet-110410-
423 132507](https://doi.org/10.1146/annurev-genet-110410-132507)

424 Lai, A., Santangelo, E., Soressi, G.P., Fantoni, R., 2007. Analysis of the main secondary
425 metabolites produced in tomato (*Lycopersicon esculentum*, Mill.) epicarp tissue during fruit
426 ripening using fluorescence techniques. *Postharvest Biol. Technol.* 43, 335–342.

427 <https://doi.org/10.1016/j.postharvbio.2006.09.016>

428 Lemos, M., Sárníková, K., Bot, F., Anese, M., Hungerford, G., 2015. Use of time-resolved
429 fluorescence to monitor bioactive compounds in plant based foodstuffs. *Biosensors* 5, 367–
430 397. <https://doi.org/10.3390/bios5030367>

431 López Camelo, A.F., Gómez, P.A., 2004. Comparison of color indexes for tomato ripening.

432 Hort. Bras. 22, 534–537. <https://doi.org/10.1590/S0102-05362004000300006>

433 Martí, R., Roselló, S., Cebolla-Cornejo, J., 2016. Tomato as a source of carotenoids and
434 polyphenols targeted to cancer prevention. *Cancers* 8, 58.
435 <https://doi.org/10.3390/cancers8060058>

436 Meléndez-Martínez, A.J., Mapelli-Brahm, P., Benítez-González, A., Stinco, C.M., 2015. A
437 comprehensive review on the colorless carotenoids phytoene and phytofluene. *Arch.*
438 *Biochem. Biophys.* 572, 188–200. <https://doi.org/10.1016/j.abb.2015.01.003>

439 Meléndez-Martínez, A.J., Stinco, C.M., Mapelli-Brahm, P., 2019. Skin carotenoids in public
440 health and nutricosmetics: The emerging roles and applications of the UV radiation-
441 absorbing colourless carotenoids phytoene and phytofluene. *Nutrients* 11, 1093.
442 <https://doi.org/10.3390/nu11051093>

443 Nagata, M., Noguchi, Y., Ito, H., Imanishi, S., Sugiyama, K., 2007. A simple
444 spectrophotometric method for the estimation of α -carotene, β -carotene and lycopene
445 concentrations in carrot acetone extracts. *Nippon Shokuhin Kagaku Kogaku Kaishi* 54, 351–
446 355. <https://doi.org/10.3136/nskkk.54.351>

447 Osorio, S., Alba, R., Nikoloski, Z., Kochevenko, A., Fernie, A.R., Giovannoni, J.J., 2012.
448 Integrative comparative analyses of transcript and metabolite profiles from pepper and
449 tomato ripening and development stages uncovers species-specific patterns of network
450 regulatory behavior. *Plant Physiol.* 159, 1713–1729. <https://doi.org/10.1104/pp.112.199711>

451 Park, H.-R., Daun, Y., Park, J.K., Bark, K.-M., 2013. Spectroscopic properties of flavonoids in
452 various aqueous-organic solvent mixtures. *Bull. Korean Chem. Soc.* 34, 211–220.
453 <https://doi.org/10.5012/bkcs.2013.34.1.211>

454 Pek, Z., Helyes, L., Lugasi, A., 2010. Color changes and antioxidant content of vine and
455 postharvest- ripened tomato fruits 45, 3.

456 Slimestad, R., Verheul, M., 2009. Review of flavonoids and other phenolics from fruits of
457 different tomato (*Lycopersicon esculentum* Mill.) cultivars. J. Sci. Food Agric. 89, 1255–
458 1270. <https://doi.org/10.1002/jsfa.3605>

459 Song, P.-S., Moore, T.A., 1974. On the photoreceptor pigment for phototropism and phototaxis:
460 Is a carotenoid the most likely candidate? Photochem. Photobiol. 19, 435–441.
461 <https://doi.org/10.1111/j.1751-1097.1974.tb06535.x>

462 Takahashi, N., Yokoyama, N., Takayama, K., Nishina, H., 2018. Estimation of tomato fruit
463 lycopene content after storage at different storage temperatures and durations. Environ.
464 Control Biol. 56, 157–160. <https://doi.org/10.2525/ecb.56.157>

465 Thai, C.N., Shewfelt, R.L., Gamer, J.C., 1990. Tomato color changes under constant and
466 variable storage temperatures: Empirical models. Trans. ASAE 33, 0607–0614.
467 <https://doi.org/10.13031/2013.31374>

468 Toor, R.K., Savage, G.P., 2006. Changes in major antioxidant components of tomatoes during
469 post-harvest storage. Food Chem. 99, 724–727.
470 <https://doi.org/10.1016/j.foodchem.2005.08.049>

471 Torres, I., Pérez-Marín, D., Haba, M.-J.D. la, Sánchez, M.-T., 2015. Fast and accurate quality
472 assessment of Raf tomatoes using NIRS technology. Postharvest Biol. Technol. 107, 9–15.
473 <https://doi.org/10.1016/j.postharvbio.2015.04.004>

474 van Roy, J., Keresztes, J.C., Wouters, N., De Ketelaere, B., Saeys, W., 2017. Measuring colour
475 of vine tomatoes using hyperspectral imaging. Postharvest Biol. Technol. 129, 79–89.

476 <https://doi.org/10.1016/j.postharvbio.2017.03.006>

477 Wünsch, U.J., Murphy, K.R., Stedmon, C.A., 2015. Fluorescence quantum yields of natural
478 organic matter and organic compounds: Implications for the fluorescence-based
479 interpretation of organic matter composition. *Front. Mar. Sci.* 2.

480 <https://doi.org/10.3389/fmars.2015.00098>

481 Zhu, Q., He, C., Lu, R., Mendoza, F., Cen, H., 2015. Ripeness evaluation of ‘Sun Bright’
482 tomato using optical absorption and scattering properties. *Postharvest Biol. Technol.* 103,
483 27–34. <https://doi.org/10.1016/j.postharvbio.2015.02.007>

484

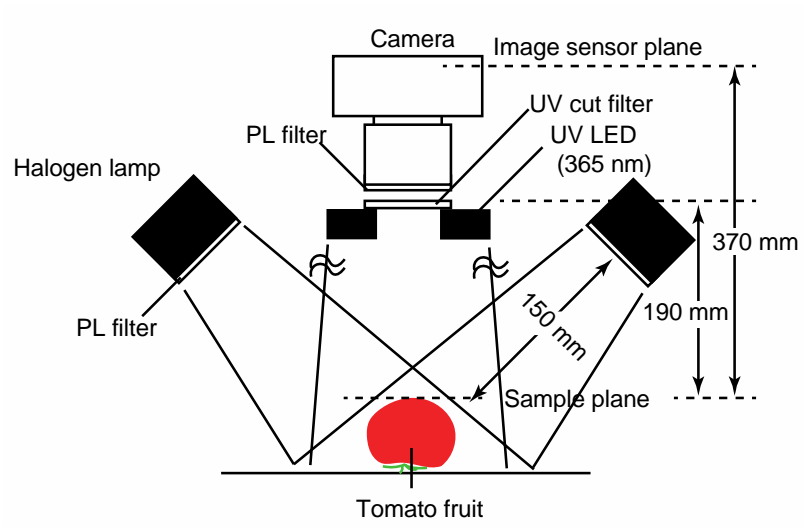


Fig. 1. Schematic diagram of the image capture setup in side view

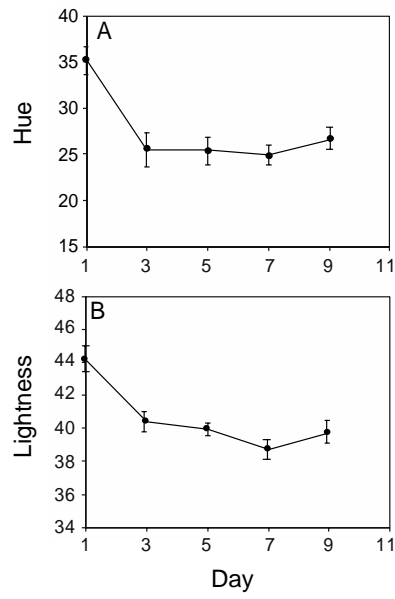


Fig. 2. Changes in hue angle (A) and lightness (B) of color of tomato measured by the colorimeter: tomatoes were harvested at the red stage and stored at 25°C until day 9 — the error bar represents the S.E. of four different fruits

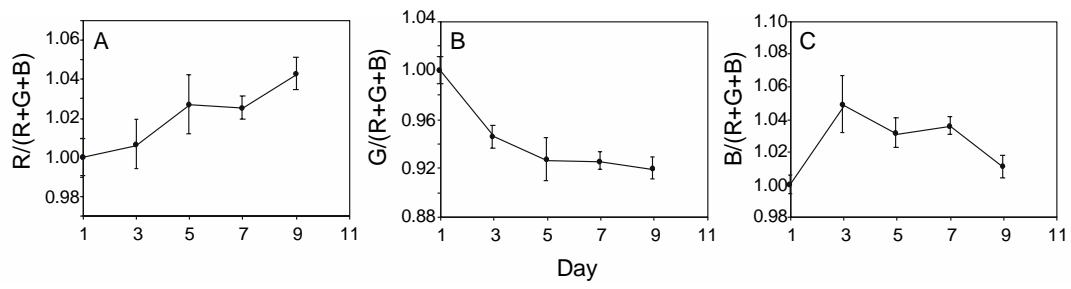


Fig. 3. Changes in relative R (A), G (B), and B (C) ratios of color of tomatoes measured by the colorimeter: tomatoes were harvested at the red stage and stored at 25°C until day 9 — the error bar represents the S.E. of four different fruits

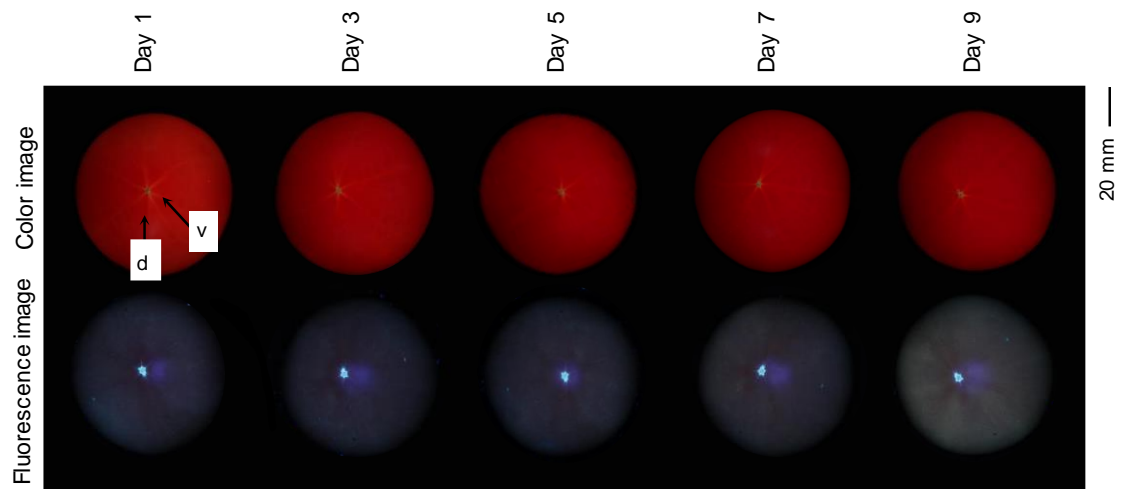


Fig. 4. Color and fluorescence images of tomatoes at the blossom end: tomatoes were harvested at the red stage and stored at 25°C until day 9 — the arrows indicate the vascular bundles (v) and the distal area (d)

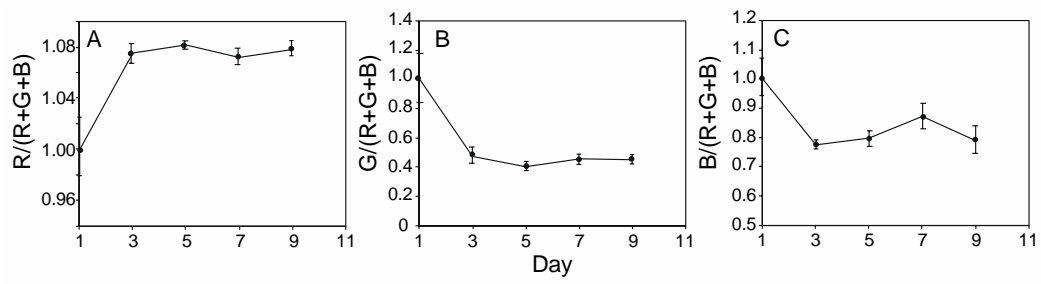


Fig. 5. Relative R (A), G (B), and B (C) ratios of color of tomatoes calculated from the color images: tomatoes were harvested at the red stage and stored at 25°C until day 9, and the colors were averaged for the blossom end without distal area — the error bar represents the S.E. of the same three fruits

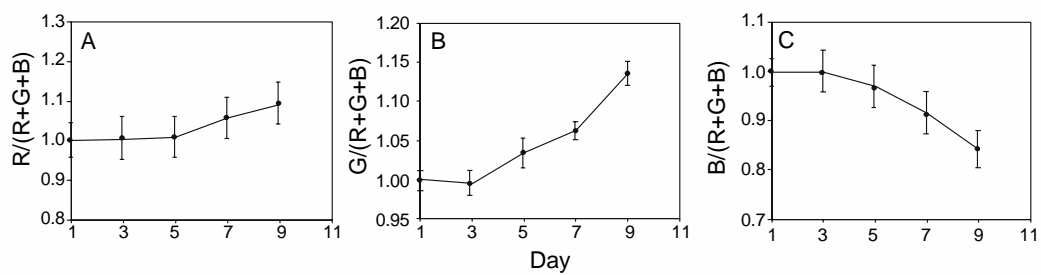


Fig. 6. Relative R (A), G (B), and B (C) ratios of fluorescence color of tomatoes calculated from the fluorescence images: tomatoes were harvested at the red stage and stored at 25°C until day 9, and the colors were averaged for the blossom end without distal area — the error bar represents the S.E. of the same three fruits

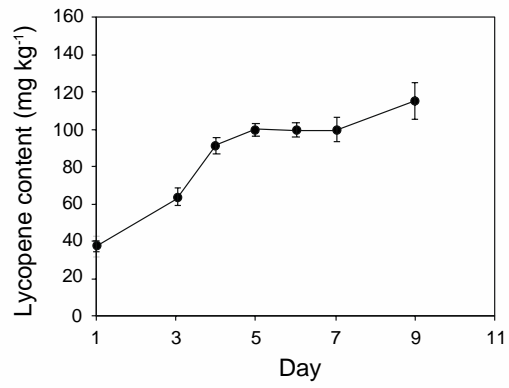


Fig. 7. Lycopene content of tomatoes harvested at the red stage and stored at 25°C until day 9 (fresh weight basis) — the error bar represents the S.E. of four different fruits

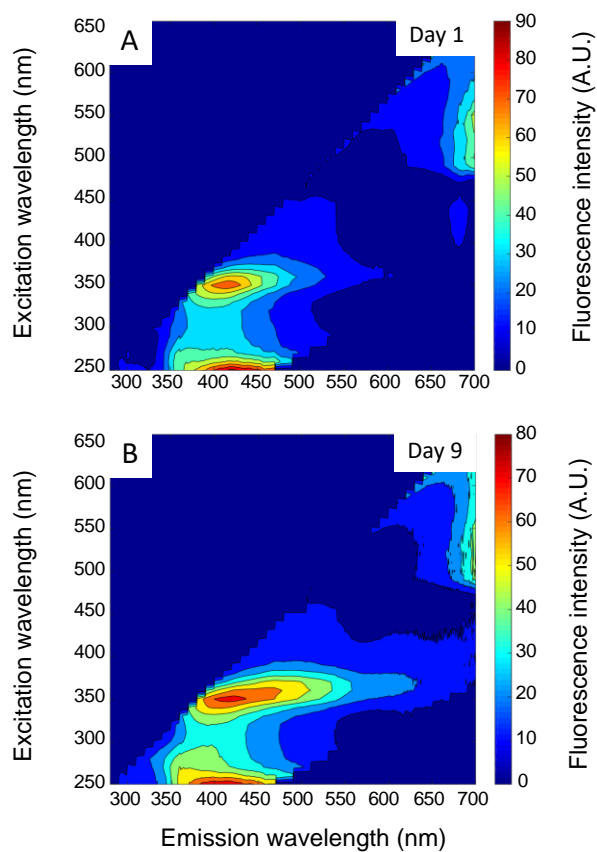


Fig. 8. Typical excitation–emission matrix (EEM) of the tomato pericarp: the tomatoes were harvested at the red stage (A) and stored at 25°C until day 9 (B), and the tomato pericarp was molded using a razor 20 mm in diameter and 3 mm in thickness — the fluorescence emission spectra at approximately 370, 470, and 540 nm were slightly distorted because of the filter in the device

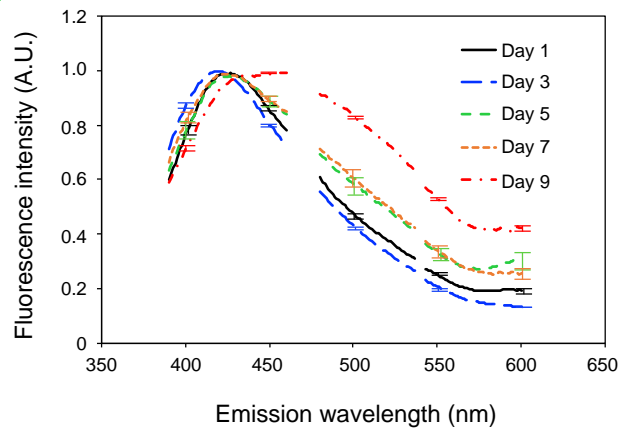


Fig. 9. Relative fluorescence emission spectra of tomato harvested at the red stage and stored at 25°C until day 9: the excitation wavelength was 360 nm, the spectra were normalized at the peak maxima, and the spectra at approximately 470 and 540 nm were cut to remove the spectral distortion caused by the filter in the device — the spectra are the mean with S.E. of four different fruits

Supplemental materials

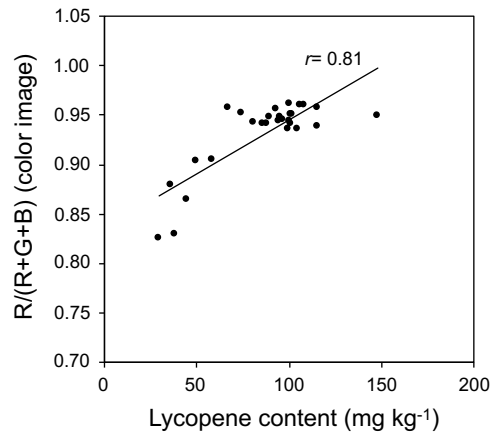


Fig. S1. Relationship between the R ratio of color image and the lycopene content during storage at 25°C (28 fruit)

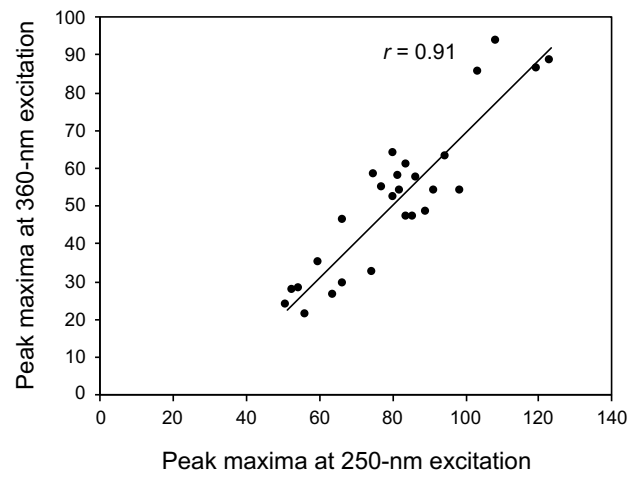


Fig. S2. Relationship between the fluorescence peak maxima at 360 and 250 nm of excitation (28 fruit)

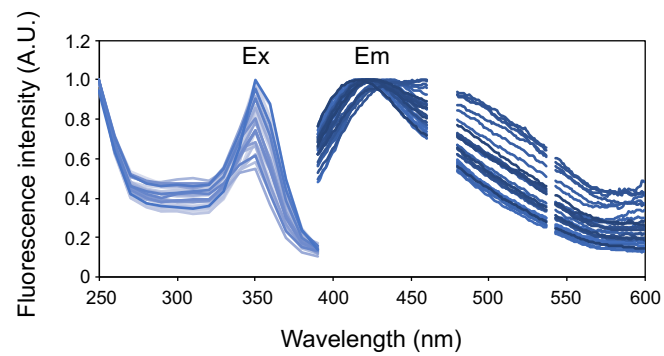


Fig. S3. Relative fluorescence excitation and emission spectra of all tomatoes measured (28 fruit): the excitation spectra were measured at 420 nm of emission, the emission spectra were measured at 360 nm of excitation, the excitation and emission spectra were normalized at the peak maxima, and the spectra at approximately 470 and 540 nm were cut to remove the spectral distortion resulting from the filter in the device